Seasonal climate summary southern hemisphere (autumn 2000): end of La Niña

R.J.B. Fawcett

National Climate Centre, Bureau of Meteorology, Australia

(Manuscript received December 2000)

Southern hemisphere circulation patterns and associated anomalies for the austral autumn (March to May) 2000 are reviewed, with emphasis given to the Pacific Basin climate indicators, and Australian rainfall and temperature patterns. During autumn the La Niña event, which had been in progress since spring of the previous year, came to an end. This was indicated by values of the Southern Oscillation Index and indices of sea-surface temperature in the tropical Pacific Ocean.

Introduction

La Niña conditions returned to the tropical Pacific region during spring 1999 and persisted through summer 1999/2000 (Della-Marta 2001). The 1999/2000 La Niña event proved shorter lived than the preceding 1998/1999 event, and weakened sufficiently rapidly during autumn 2000 that it had concluded by the end of the season. Even so, autumn rainfall was above to very much above average across most of Australia, with much of the northwest coast receiving highest on record autumn totals. The widespread wet conditions were accompanied by below average seasonal maximum temperatures.

This summary reviews the southern hemisphere and equatorial climate patterns of autumn 2000, with particular attention given to the Australasian and Pacific regions. The main sources of information for this report are the *Climate Monitoring Bulletin* (Bureau of Meteorology, Australia) and the *Climate Diagnostics Bulletin* (Climate Prediction Center (CPC), Washington). Further details regarding sources of data are given in the Appendix.

Corresponding author address: Dr R.J.B. Fawcett, National Climate Centre, Bureau of Meteorology, GPO Box 1289K, Melbourne, Vic. 3001, Australia.

Pacific Basin climate indices

The Troup Southern Oscillation Index (SOI)*

The set of three positive monthly values (+12.8, +5.1 and +12.9) for the Troup Southern Oscillation Index (SOI) during summer 1999/2000 (Della-Marta 2001) was followed by +9.4 (March), +16.8 (April) and +3.8 (May). The drop in the SOI towards the end of autumn, signifying the end of the positive phase of the Southern Oscillation and due more to changes in atmospheric pressure at Darwin than changes at Tahiti, was subsequently reinforced by negative values for the first two months of winter. It is interesting to note that the progression of the SOI from February to May showed considerable similarity to the values of February to May 1999. Figure 1 shows the monthly SOI values from January 1996 to May 2000. A five-month moving average curve is superimposed on the graph.

Outgoing long wave radiation

Figure 2, adapted from the Climate Prediction Center, Washington (CPC 2000), shows the monthly stan-

*The Troup Southern Oscillation Index (SOI) used in this article is ten times the monthly anomaly of the difference in mean sea-level pressure between Tahiti and Darwin, divided by the standard deviation of that difference for the relevant month, based on a sixty-year climatology (1933 - 1992).

Fig. 1 **Southern Oscillation Index, from January 1996 to May 2000. Means and standard deviations used in the computation of the SOI are based on the period 1933-1992.**

Fig. 2 **Standardised anomaly of monthly outgoing long wave radiation averaged over the area 5°N - 5°S and 160°E - 160°W, from January 1996 to June 2000. Negative (positive) anomalies indicate enhanced (reduced) convection and rainfall. Anomalies are based on a 1979-95 base period mean. After CPC (2000).**

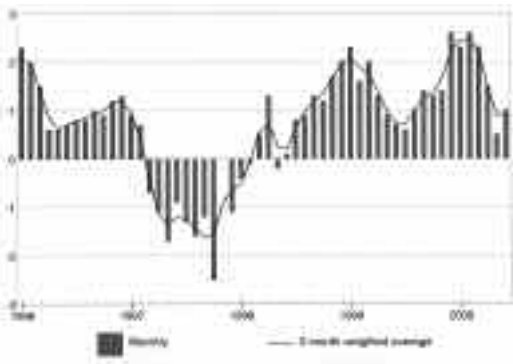

dardised anomaly of outgoing long wave radiation (OLR) from January 1996 to June 2000, together with a three-month moving average. These data, compiled by the CPC, are an indication of the amount of long wave radiation emitted from an equatorial region centred about the date-line (5°S to 5°N and 160°E to 160°W). Tropical convection in this region is particularly sensitive to changes in the phase of the Southern Oscillation. During warm (El Niño) events, convection is generally more prevalent resulting in a reduction in the intensity of the OLR due to the lower effective black-body temperature, while the reverse applies in cold (La Niña) events. Values of this index for March, April and May were consistent with the waning La Niña event. In fact, the pattern of values for the last two years had been quite consistent with the broader picture of two consecutive La Niña events. OLR anomalies in the sampled region were marginally stronger in the second of the two events. The OLR anomalies in both these events were considerably stronger and more persistent than those of the El Niño event of 1997/98, which immediately preceded these two La Niña events. The El Niño was the much stronger ENSO event overall, however.

Oceanic patterns

Sea-surface temperatures

Figure 3 shows the autumn 2000 sea-surface temperature (SST) anomaly in degrees Celsius (°C). The contour interval is 1°C. Positive anomalies are shown in orange and red shades, while negative anomalies are shown in blue shades. The tropical Pacific Ocean in autumn still showed a recognisable La Niña pattern, with negative anomalies surrounded by a rotated 'V' of positive anomalies. In the eastern tropical Pacific however, the negative anomalies had shifted considerably into the northern hemisphere, to be replaced by mostly positive anomalies along the equator. Anomalies in the range –1 to –2°C persisted in the central tropical Pacific, between 180° and 140°W. The NINO3 and NINO4 SST weekly time series (not shown), as calculated by the National Meteorological and Oceanographic Centre, Melbourne, both showed the 1999/2000 La Niña event as peaking around January/February. The SST index in the NINO3 region had returned to neutral values by March (consistent with the seasonal pattern described above), while in the NINO4 region it took until May.

In terms of the NINO4 index, the La Niña events of 1998/1999 and 1999/2000 were of approximately equal magnitude. In contrast, the earlier event showed a much weaker presence in the NINO3 region.

For the extratropical southern hemisphere, the most noticeable feature of the analysis shown in Fig. 3 is the near complete band of negative anomalies in the high latitudes surrounding Antarctica. This pattern is only broken in the southwest Atlantic Ocean, southeast of southern South America. Around Australia, the anomalies were mostly weak, apart from along the southwest coast of Western Australia, where they exceeded +1°C. These latter anomalies arose during November 1999, and intensified considerably during December.

Fig. 3 Anomalies of sea-surface temperature for autumn 2000 (°C)

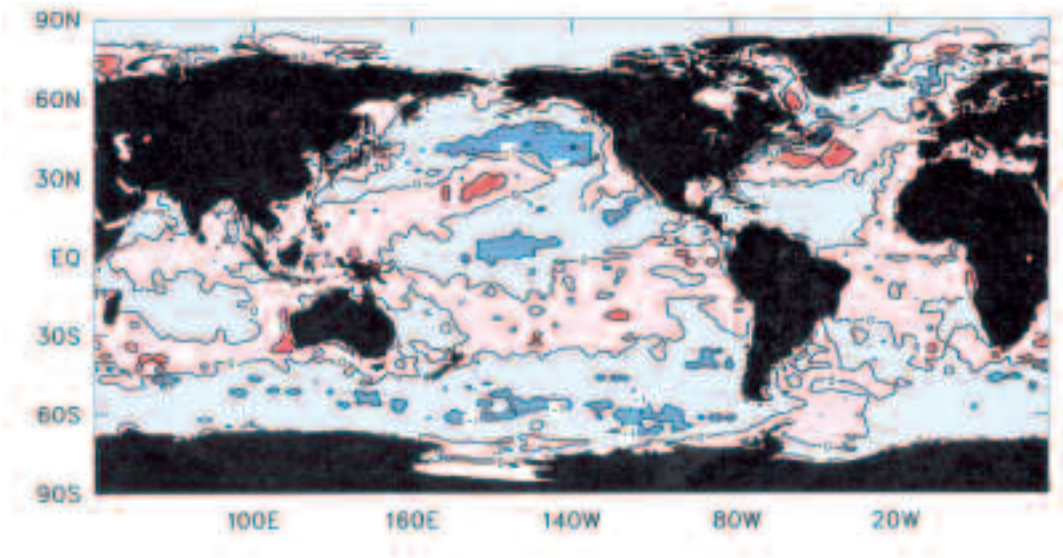

Subsurface patterns

Figure 4 shows the anomaly in metres of the depth of the 20°C isotherm along the equatorial Pacific Ocean between January 1995 and May 2000. This isotherm is generally situated very close to the equatorial ocean thermocline, the region of greatest temperature gradient with respect to depth. The thermocline can also be regarded as the boundary between the upper ocean warm water and the deeper ocean cold water. An abnormally shallow thermocline in the eastern Pacific Ocean is characteristic of La Niña events. Positive anomalies correspond to the 20°C isotherm being deeper than average, and negative anomalies to it being shallower than average.

The picture at the end of autumn showed moderate positive anomalies in the western tropical Pacific, with only minor indications of eastward propagation. The decline in the subsurface signal of the cool event in the central and eastern Pacific was well advanced by the start of autumn, and by the end of the season it had returned to neutral values. Overall, the 1999/2000 cool event showed a much weaker and shorter signal than the preceding 1998/99 event.

Fig. 4 Time-longitude section of the monthly anomalous depth of the 20°C isotherm at the equator from January 1995 to May 2000. The contour interval is 10 m.

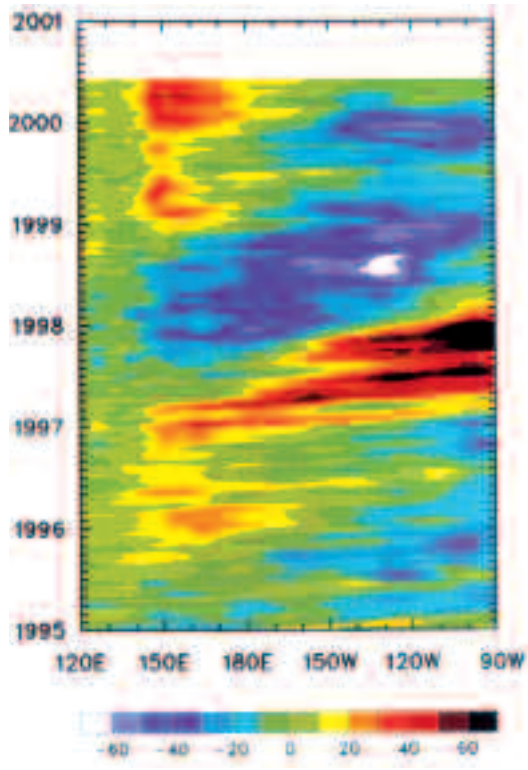

Surface analyses

The autumn 2000 mean sea-level pressure (MSLP) across the southern hemisphere is shown in Fig. 5, with the associated anomalies shown in Fig. 6. These anomalies are the departures from an eleven-year (1979-1989) climatology obtained from the European

Fig. 5 Mean sea-level pressure for autumn 2000 (hPa).

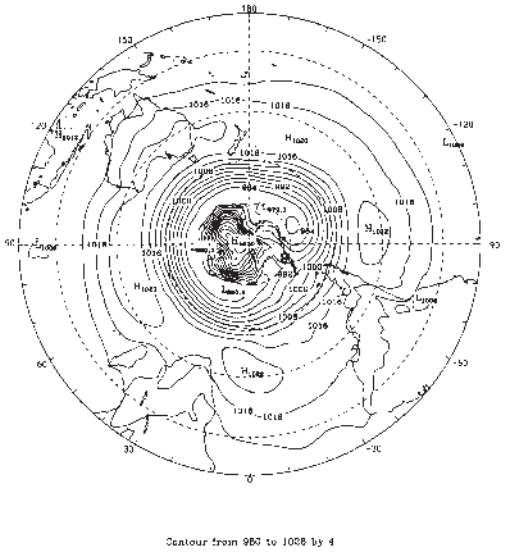

Fig. 6 Anomalies of the mean sea-level pressure from the 1979-89 ECMWF climatology, for autumn 2000 (hPa).

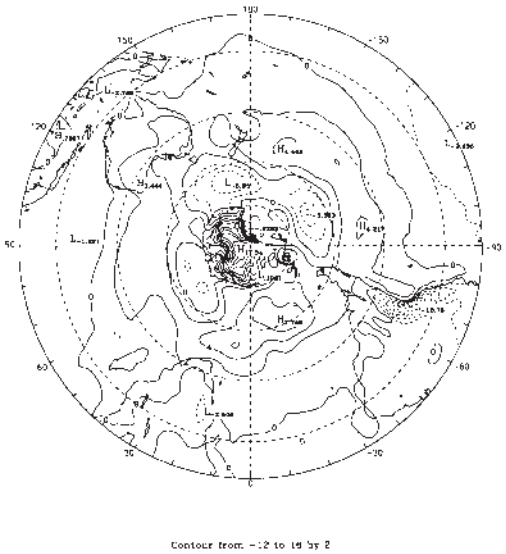

Centre for Medium-range Weather Forecasts (ECMWF). The MSLP analysis itself has been computed using data obtained from the Bureau of Meteorology's Global Assimilation and Prediction (GASP) model daily 2300 UTC analyses. The contours in Fig. 5 are spaced at 4 hPa intervals between 980 hPa and 1028 hPa, while the contours in Fig. 6 are spaced at 2 hPa intervals between –12 hPa and +16 hPa. The low pressure anomaly over South America in Fig. 6 is a persistent feature, and appears to result from a systematic difference between the GASP and ECMWF models, rather than as a meteorological consequence of the current state of the El Niño-Southern Oscillation.

In the Antarctic region, the MSL pressure anomalies (Fig. 6) had some similarity to those of autumn 1999 (de Hoedt 2000). They consisted of a stronger than average anticyclone over the Antarctic continent itself, with three broad centres of below average pressures north of the polar trough. These negative anomalies were located in the southern Indian Ocean, in the Southern Ocean south of New Zealand and in the southeastern Pacific Ocean. A similarly sized but positive anomaly in the southern Atlantic Ocean completes the pattern.

Moving further equatorwards, a band of positive anomalies stretching around most of the southern Indian and Pacific Oceans between 30° and 50°S indicates a subtropical ridge which was more intense than normal. MSLP anomalies were above average over almost all of Australia, peaking at +3.4 hPa in the southwest corner of the continent.

Mid-tropospheric analyses

Figures 7 and 8 show the mean and anomalous geopotential height patterns at 500 hPa respectively for autumn 2000. The contours in Fig. 7 are spaced at 80 geopotential metre intervals from 4960 gpm to 5840 gpm, while the contours in Fig. 8 are spaced at 40 gpm intervals from –80 gpm to 80 gpm. The MSLP anomaly patterns described above are largely replicated at the 500 hPa level, although in smoothed form. The main difference is that the above-average Antarctic anticyclone is no longer present at this level, with negative height anomalies over more than half of the continent.

Blocking

Figure 9 is a time-longitude section of the daily southern hemisphere mid-level Blocking Index,

$$BI = 1/2[(u_{25}+u_{30}) - (u_{40}+2u_{45}+u_{50}) + (u_{55}+u_{60})] \quad \ldots 1$$

Here, u_λ indicates the 500 hPa level zonal wind component at λ degrees of southern hemispheric latitude ranging from 0° at the equator to +90° at the South Pole, under the usual convention that positive (negative) values of u_λ correspond to westerly (easterly) winds. The blocking index measures the strength of

Fig. 7 Mean 500 hPa geopotential height for autumn 2000 (gpm).

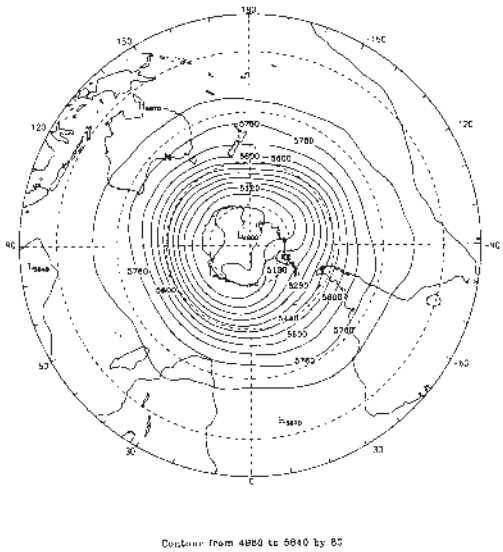

Fig. 8 Anomalies of 500 hPa geopotential height from the 1979-89 ECMWF climatology, for autumn 2000 (gpm).

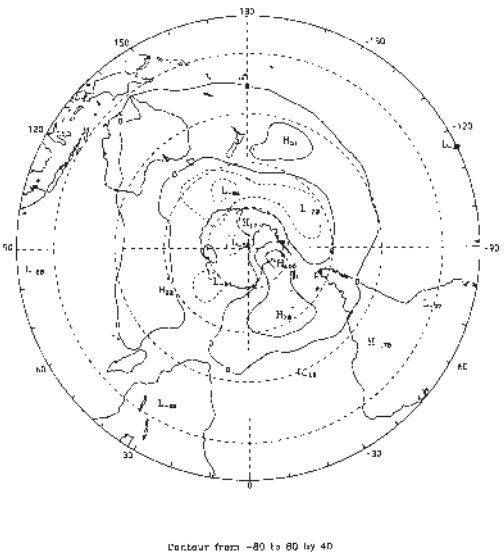

the 500 hPa flow at the mid-latitudes (40°S to 50°S) relative to that at subtropical (25°S to 30°S) and high (55°S to 60°S) latitudes. The horizontal axis of Fig. 9 measures degrees of longitude east of the Greenwich Meridian. The top of the figure represents the start of autumn, with the bottom of the figure representing the end of autumn.

Fig. 9 Autumn 2000 daily blocking index at the 500 hPa level: time-longitude section. Day 1 is 1 March 2000.

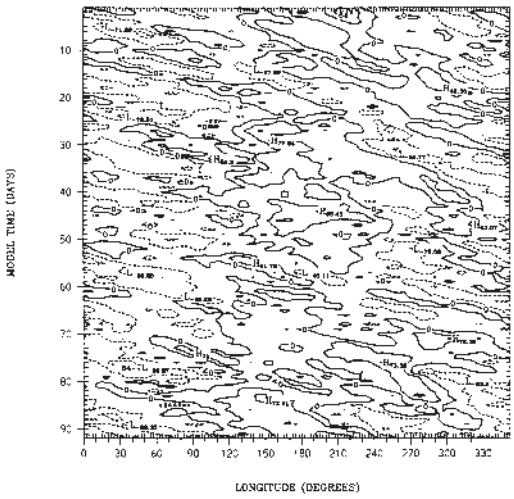

Taken across the entire season in the form of a seasonal mean (not shown), blocking was close to average between 60°E and 155°E, but slightly below average between 155°E and 80°W. Climatologically, maximum blocking for the season occurs at about 170°E, although in autumn 2000 the maximum was located slightly further west, at about 160°E.

Erratum

The National Climate Centre has recently become aware that its calculated blocking index values as published in the *Climate Monitoring Bulletin* (CMB) from January 1993 to July 2000 have been inconsistent with the published definition (see, for example, de Hoedt 2000), here reproduced in Eqn 1. The error has been two-fold, involving firstly an unwanted weighting of the zonal wind components with the cosine of the latitude and secondly an inconsistent treatment of the averaging process across the three latitudinal bands given above. A comparison of the correct results for August 2000 (appearing in the August issue of the CMB) and the results of the hitherto used (incorrect) method show a substantial change in the actual values of the blocking index, but relatively little change in the qualitative features of the resulting graph (with respect to both the longitudinal variation around the southern hemisphere and the departure from the ECMWF climatological values). The erroneous method of calculation was used on both the real-time BI values and the climatological values, and applied equally to the monthly averages and the daily Hovmöller charts.

In respect of these seasonal climate summaries in the *Australian Meteorological Magazine*, the National Climate Centre believes that all summaries from spring 1992 to summer 1999/2000 exhibit the same error.

Low and upper-level winds

Low-level (850 hPa) and upper-level (200 hPa) wind anomalies for autumn are shown in Figs 10 and 11 respectively. These also have been computed from the Bureau of Meteorology's GASP model analyses. The seasonal low-level wind anomalies were easterly in the western tropical Pacific region, although the corresponding monthly anomalies were much weaker in May than in March and April. There were also signs of enhanced trade wind activity in both hemispheres for the central Pacific. This, together with enhanced westerlies in the upper levels (Fig. 11) over the central and eastern equatorial Pacific Ocean, point to an enhanced Walker circulation, consistent with the values of the SOI reported above. In contrast, the upper-level anomalies across the Indian Ocean were consistently easterly from 20°S to 20°N.

Across Australia, the low-level seasonal anomalies were generally weak; northeasterly over most of Western Australia and generally northerly over Queensland. The upper-level anomalies were easterly over northern half of the continent, changing to westerly over Tasmania.

Australian region

Rainfall

Figure 12 shows the autumn rainfall totals for Australia, while Fig. 13 shows the autumn rainfall deciles, based on gridded rainfall data for the period 1900 - 2000. The effects of the La Niña event show up dramatically across most of Australia. Almost the entire northwest coast received very much above average (decile 10) rainfall during autumn, with widespread areas receiving 'highest on record' totals for the season. These high rainfalls were due in part to tropical cyclones *Steve* in March and *Rosita* in April. The seasonally high rainfall also extended in a band across central Australia and down into central New South Wales, while tropical cyclones *Tessie* and *Vaughan* brought high rainfalls to northeastern Australia during April.

The area of low rainfall in southwest Western Australia was almost entirely due to the very much below average (decile 1) rainfalls in May, marking a poor start to the southern wet season in that area. In fact, some parts of southern WA received 'lowest on record' May totals. Average rainfalls in southern Victoria and below average rainfalls in eastern Tasmania contributed to the continuation of drought conditions in those areas. The low rainfall in southeast Queensland followed average to below average totals in this region during summer (Della-Marta 2001).

Fig. 10 Anomalies of the vector wind at the 850 hPa level from the 1979-89 ECMWF climatology, for autumn 2000 (m s^{-1}).

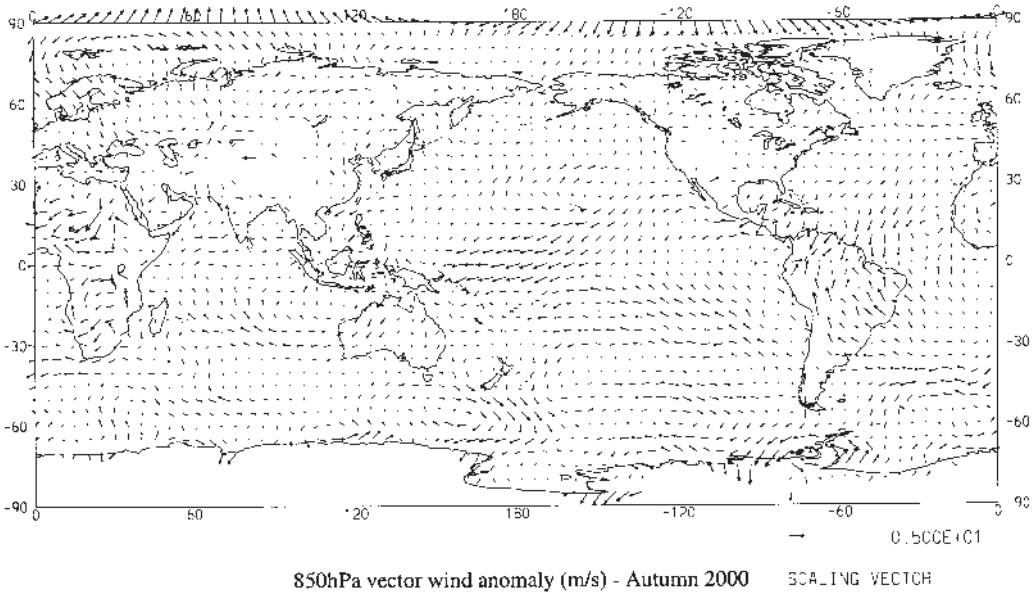

Fig. 11 **Anomalies of the vector wind at the 200 hPa level from the 1979-89 ECMWF climatology, for autumn 2000 (m s^{-1}).**

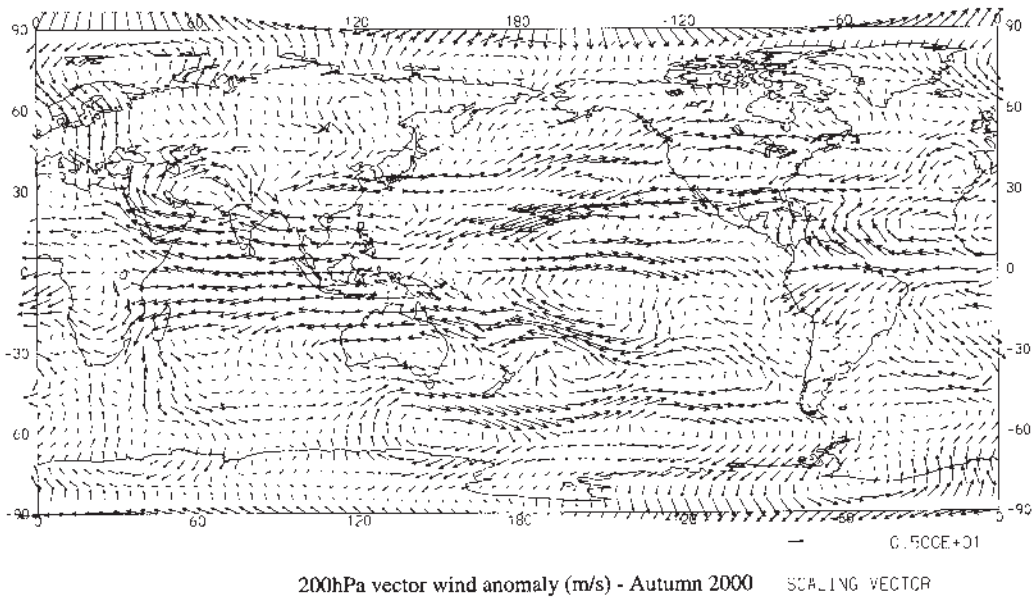

Fig. 12 **Rainfall totals over Australia for autumn 2000 (mm).**

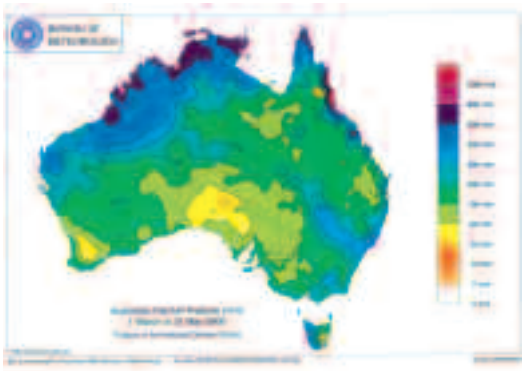

Fig. 13 **Deciles of rainfall over Australia for autumn 2000, based on the 101-year 1900-2000 base period.**

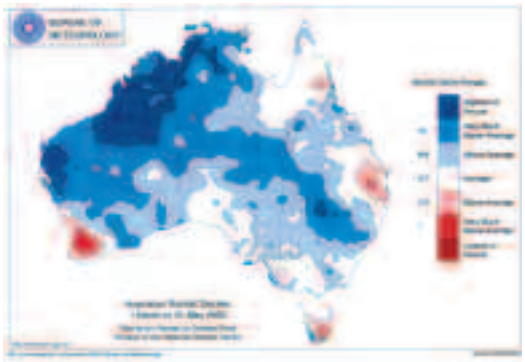

Temperatures

Figures 14 and 15 show the maximum and minimum temperature anomalies respectively for autumn 2000. The anomalies have been calculated with respect to the 1961-90 period. Maximum temperatures were below average across most of the continent. The substantial negative anomalies were largely due to persistent wet and cloudy conditions, with the disposition of the anomalies overall showing a substantial degree of similarity to the rainfall anomalies (Fig. 13). The strongest anomalies were over Western Australia, with a wide area experiencing seasonal anomalies between –3 and –4°C. In Tasmania, the anomalies were positive almost everywhere.

Arguably, the monthly maximum temperature anomaly for May came closest to the overall seasonal pattern. April's anomalies showed a similar pattern, but for March the anomalies in the east were much more patchy. The strongest monthly anomalies were in Western Australia during March, with a large area in the southern half of the State recording anomalies in excess of –5°C and reaching –6°C in a few places. A –5°C anomaly was recorded at Giles for April. Averaged across Western Australia, autumn 2000 had the lowest seasonal maximum temperature of the post-1949 period. An analogous claim could be made for the Northern Territory.

Minimum temperatures were also below average for most of Western Australia, where the strongest seasonal anomalies were recorded, but above average for most of the rest of the country. The monthly anom-

Fig. 14 Autumn 2000 maximum temperature anomalies (°C) for Australia based on a 1961-90 mean.

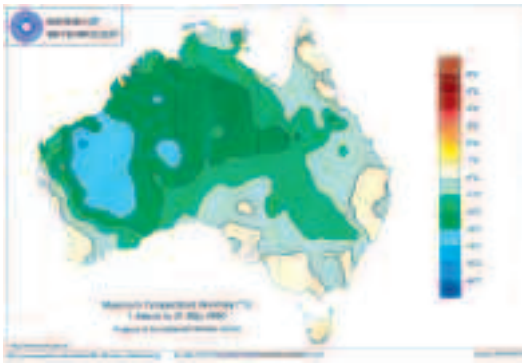

Fig. 15 Autumn 2000 minimum temperature anomalies (°C) for Australia based on a 1961-90 mean.

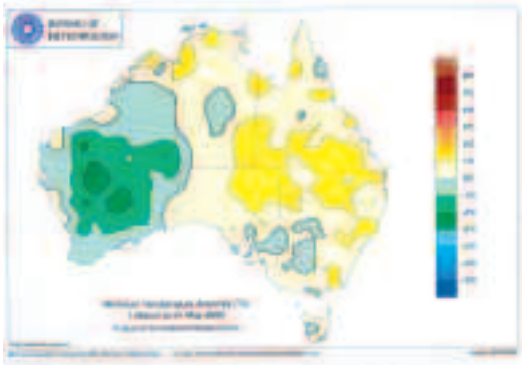

aly pattern for April showed similarities to the overall seasonal pattern, although with stronger anomalies in some central and eastern parts. Intense monthly anomalies in the range –3 to –5°C were recorded across central Western Australia during May.

References

Della-Marta, P. 2001. Seasonal climate summary southern hemisphere (summer 1999/2000): A second successive weak cool episode (La Niña) reaches maturity. *Aust. Met. Mag., 50*, 65-75.

de Hoedt, G. 2000. Seasonal climate summary southern hemisphere (autumn 1999): a decline in weak cold episode conditions in the tropical Pacific. *Aust. Met. Mag., 49*, 51-8

Bureau of Meteorology 2000. *Climate Monitoring Bulletin,* March, April, May, June and July issues. National Climate Centre, Bur. Met., Australia.

Climate Prediction Center 2000. *Climate Diagnostics Bulletin*, March, April and May 2000. US Department of Commerce, National Oceanic and Atmospheric Administration, Washington D.C.

Appendix

The main sources for data used in this review were:
National Climate Centre, *Climate Monitoring Bulletin*. Obtainable from: National Climate Centre, Bureau of Meteorology, GPO Box 1289K, Melbourne Vic. 3001, Australia.

Climate Prediction Center (CPC), *Climate Diagnostics Bulletin*. Obtainable from: Climate Prediction Center (CPC), National Weather Service, Washington D.C., 20233, USA.